Small-Scale FDM Prototyping for Early Design of Deployable Structures: Telescoping and Origami-Inspired Mechanism Case Studies
by Chloe Yang

1. Introduction

1.1 The Larger Engineering and Prototyping Problems

Collapsible housing systems have applications in disaster relief, temporary accommodation, military operations, and even potential space habitation. These uses require structures that can be compressed for transportation, deployed efficiently, and remain stable and durable when occupied; as such, designing mechanisms that satisfy all of these requirements presents a continuing engineering challenge. However, constructing large or occupiable prototypes requires substantial resources and may also create safety risks. Small-scale prototyping in early development can thus offer a practical method for exploring collapsible mechanisms before attempting full-scale construction.

Fused deposition modeling (FDM), a common form of 3D printing, is particularly useful for small-scale prototyping. Complex components can be produced directly from CAD files and modified relatively quickly and inexpensively. Instead of manufacturing a complete structure, a designer can print a simplified version of a mechanism, test it, observe its failures, and change the digital design before producing another version. This iterative process can reduce the material, time, and expense required to investigate multiple design choices.

At the same time, small-scale 3D printing has significant limitations; a plastic model does not experience the same forces as a full-sized structure, and common printing filaments do not represent the materials that would be used in an actual building. Therefore, successful operation of a printed model cannot prove that the same design would be safe or practical at architectural scale.

1.2 Case Study

Then, we ask: how effectively can inexpensive FDM prototypes identify mechanism-specific design parameters, as well as tradeoffs in deployable structure geometry, before larger-scale fabrication? This study examines both the value and the limitations of small-scale 3D printing through the development of two collapsible structural concepts, as well as investigating the robustness of the two design concepts for future development.

The first concept uses a Miura-ori-inspired folding pattern from origami, which collapses vertically downwards in a singular motion. The second concept uses a telescoping mechanism consisting of curved shells that nest inside one another and move along rails in a horizontal fashion.

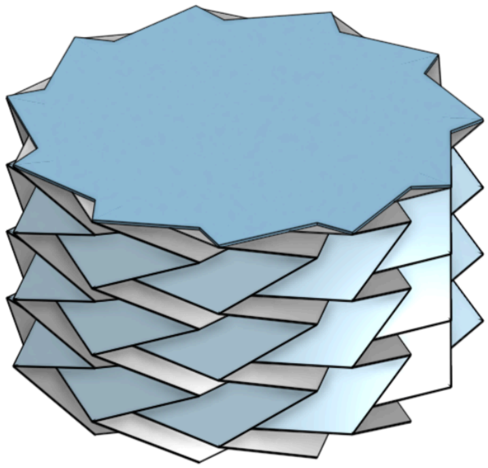

Fig1. Miura Model (vertical compression)

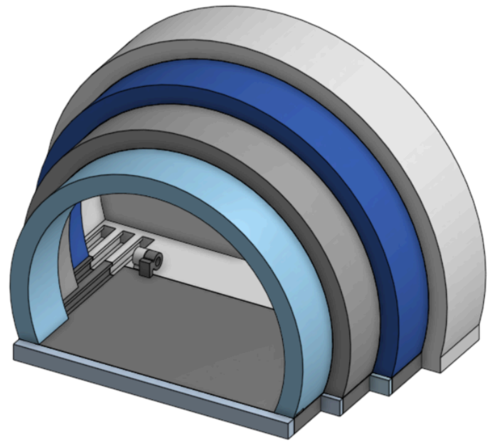

Fig2. Telescoping Model (linear compression)

The purpose of this project is not to demonstrate a complete or occupiable collapsible building. The models are treated as mechanism studies as well as evaluating the effectiveness of FDM small-scale prototyping. Specifically for this case study, we ask: can the prototype identify important design parameters?; can it reveal tradeoffs between competing design objectives?; can it reveal failure modes or interactions that are difficult to see in CAD alone?; and can it reveal important comparisons and information about the two design geometries for future large-scale development?

The hypothesis is that small-scale 3D printing cannot accurately predict the strength, durability, or safety of a full-scale collapsible structure, but it can serve as a useful early-stage engineering tool. In particular, it can reveal the feasibility and robustness of specific geometries (in this case, the compactness, durability, and consistency of a collapsing model), movement and component interaction, and provide quick results to assist iteration.

2. Background

2.1 Prototyping and 3D Printing

Fused-filament fabrication (3D printing) is a form of additive manufacturing in which thermoplastic filament is melted and deposited layer by layer according to a digital model. Because a part can be produced directly from a CAD file without first manufacturing a mold, 3D printing is useful for early design development: a model can be printed, tested, modified digitally, and printed again in a quick and easy fashion. Additive manufacturing can also produce complex and customized geometries that may be difficult to construct using conventional tools [1].

3D printing is thus often used in prototyping. A prototype does not always need to reproduce every feature of the intended product, and in fact, designers often use different kinds of prototypes to investigate different attributes of a design. So, 3D printing can be a useful tool at the small-scale level.

In this study specifically, for example, the models are primarily mechanical prototypes and are intended to investigate how the two structures collapse and expand. 3D printing made it possible to test the physical movement of the telescoping and origami-inspired mechanisms at a manageable scale. CAD could show the intended positions of the components, but a physical model was needed to reveal problems such as surface friction, insufficient clearance, panel interference, hinge stiffness, and more. Because design changes could be made in CAD and then reprinted, the process supported repeated cycles of design, fabrication, observation, and revision, undergoing quick and inexpensive iteration.

The usefulness of a prototype should be judged by whether it answers the question it was designed to investigate. In this project, a prototype is considered useful if it identifies a design problem, reduces uncertainty, supports a measurable comparison, or provides information that can guide the next design version.

2.2 Collapsible Housing

Collapsible housing belongs to the broader category of deployable architecture: structures designed to change between a compact transportation state and a larger usable state. Research has identified transitional and collapsible shelters as particularly essential for post-disaster housing [2], making collapsible housing a significant area to research. Meanwhile, collapsible housing can also be used for many other purposes, such as potential space habitation.

A successful collapsible housing system must meet several competing requirements: it should occupy little space during transportation, expand into a useful interior volume, require few people or tools to deploy, and remain stable after deployment. Two mechanisms that may address these requirements are origami-inspired folding and telescoping: both allow a structure to become more compact, although they achieve this transformation in fundamentally different ways.

Origami-inspired structures use geometric patterns of connected panels and fold lines that can collapse and deploy rapidly. Previous research has specifically considered origami for deployable shelters: Verzoni and Rais-Rohani developed and analyzed multiple origami-inspired shelter concepts, showing that compound folding patterns could be incorporated into thick-walled shelter concepts [3]. Kim et al. designed a collapsible and expandable housing prototype for space exploration using origami principles, proving mechanical viability and quick actuation [4].

The Miura-ori fold in origami is one of the most common origami-inspired structures to be used in engineering. Ye et al. (2023) used multimaterial FDM 3D printing, wrapping rigid PLA panels with flexible TPU, to develop a Miura sheet that could withstand an 11000x load and fold more than 100 times without visible strain. [5] Sun et al. similarly created a Miura sheet using additive manufacturing (3D printing) that could withstand mechanical load even after 1000 repeated deployment cycles. [6]

Telescoping mechanisms provide a second possible approach to collapsible housing. A telescoping mechanism consists of rigid sections that fit inside or overlap one another and slide between collapsed and expanded positions. Unlike an origami-inspired structure, a telescoping design does not require its main surfaces to bend, and components may remain rigid throughout the entirety of the collapsing process.

The two prototypes in this study were designed to investigate these contrasting approaches. The telescoping model uses nested curved shells that slide along rails, while the Miura-ori-inspired model changes shape through the folding of connected panels. Studying both mechanisms makes it possible to compare two different methods of reducing a structure's transportation volume: translating rigid components and folding connected surfaces.

2.3 Materials Research

The two primary filaments used in the project were polylactic acid (PLA) and polyethylene terephthalate glycol-modified (PETG). PLA is generally the more rigid of the two materials and is widely used because it is relatively easy to print and can produce dimensionally consistent parts. These characteristics make PLA useful for components that are intended to retain their shape, such as shells, rails, stops, and guides. Its rigidity also means that thin PLA components may fracture rather than tolerate repeated bending.

PETG is generally less stiff and capable of greater deformation before failure. Martins et al. compared fused-filament-fabricated PLA and PETG specimens and found that PLA had a higher average Young's modulus, a measurement related to material stiffness. In their tests, PLA had a modulus of approximately 2,350 MPa, compared with approximately 1,200 MPa for PETG. PETG reached a greater average strain before failure: approximately 6.5%, compared with 4.3% for PLA [7].

Based on these characteristics, PLA was selected for the telescoping prototype. Its rigidity helped the curved shells and rails maintain their intended geometry during sliding. PETG was selected for the Miura-ori-inspired prototype because the fold regions needed to bend rather than remain completely rigid, and because the 3D printer available did not support TPU filament, which is even softer. The PETG panels and hinges could therefore be used to explore how fold thickness and print orientation affected the movement of the model.

This material selection does not constitute a controlled comparison between PLA and PETG. The materials also represent the mechanisms rather than the materials of a future full-scale building. 3D printing is therefore efficient in this project mainly as a rapid-prototyping process, reducing the time and resources required to move from a digital design to a testable physical mechanism.

3. Design Development

3.1 Design objectives

Three main design goals were established for the prototypes—each model was expected to move between a clearly defined collapsed state and expanded state; complete its movement without major component interference; and be capable of repeated deployment without immediate failure. Beyond this, smaller design goals included robustness and durability during and after expansion; a complete locking system; and having as small a collapsed state as possible without interfering with any other design goals.

Two different mechanisms were designed: the telescoping and origami-inspired mechanisms, as outlined above. These two approaches were mainly selected due to their contrasting features and unique attributes that presented engineering challenges in large-scale applications (linear sliding and vertical rotational folding). These were also designs that could feasibly be fabricated through quick and accessible 3D-printing methods. Thus, they were selected in order to demonstrate how 3D printing can be used as a physical demonstration and tool for identifying design changes.

Features necessary for complete housing like insulation, weatherproofing, windows, and utilities, were outside the scope of the project. It is also important to note that the locking mechanisms were not the specific focus of the studies and are not claimed to be the most sophisticated or robust mechanisms possible.

3.2 Telescoping

The telescoping prototype consisted of four curved shell sections arranged from largest to smallest. In the collapsed state, the smaller shells nested inside the larger shells. During deployment, the shells moved outward along three rails positioned on each side of the base. These shells were all completely rigid.

For a locking mechanism, the design ultimately utilized a gravity-based pin lock, in which a pin dropped into a hole at the bottom when the shell fully deployed. The pin could be lifted using a handle on the outside of the shell, allowing the shell to slide back in afterwards. Two separate floor pieces were modeled, where the larger piece would fold up and down around a simple hinge system depending on whether the shells were deployed or not. Stops were added to the front of the rails to prevent shells from sliding out completely.

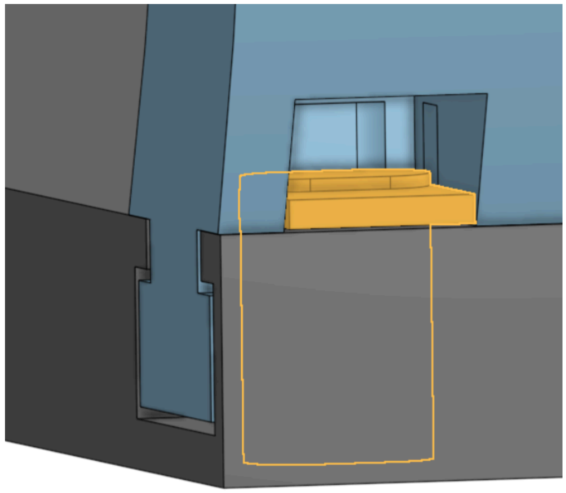

Fig3. Pin in the locking position

3.3 Miura

The second prototype explored a folding method based on the Miura-ori origami fold pattern; the Miura fold was selected for the reasons outlined prior, as it has been proven to be a robust engineering mechanism. Its surface was divided into repeated panels connected by thinner flexible regions, and the panels followed a general parallelogram shape.

The panels and fold regions were printed as connected components using PETG. The main panels were made thick enough to retain their shapes, while the fold regions were made thinner (with chamfer connections) to concentrate bending along intended lines. Instead of printing the entire model together, the roof and eleven flat strips were printed individually, then mechanically assembled by hand, due to the model's need for flexibility.

To keep the model in its collapsed state, a tube extended from the floor and the lid contained a hole that would allow the tube to extend through. The tube contained multiple through-holes at different heights: 5, 10, 15, and 20 mm (to see the maximum distance the mechanism could compress). Then, a long pin spanning the width of the lid was slid through the lowest through-hole the model could compress under, in order to lock the model in its compressed state. If the model needed to be expanded again, the pin was taken out. A similar mechanism was employed to lock the model in its most expanded state. Two tubes raised on either side of the mechanism similarly contained multiple levels of through holes, and a pin was slid into the highest through-hole the model could expand above.

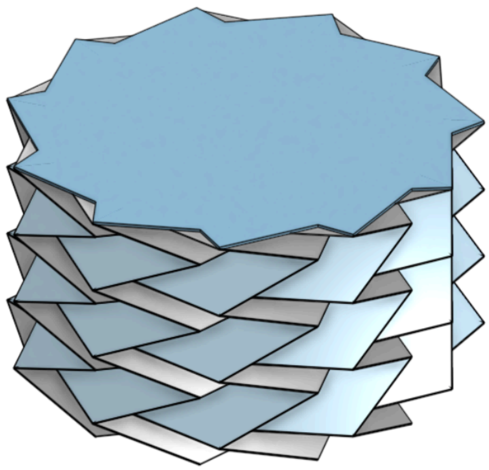

Fig4. Full Assembly (sans locking mechanisms)

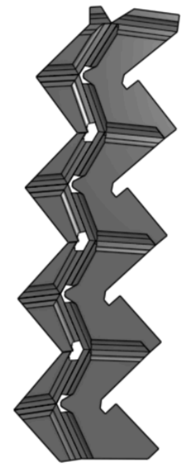

Fig5. Single Strip Configuration

4. Testing & Results

4.1 Methods

Models were designed on cloud-based CAD software Onshape, and printed on a Bambu A1 Mini 3D printer. The Miura model was fabricated using flat panels with Generic PETG. 11 of these panels were printed and glued together (with the thin rectangular panels on the left) using Gorilla Super Glue Gel. The top and bottom were printed separately and the top lid was glued using the upper tabs shown in the single panel strip. The telescoping model was printed using Generic PLA, with the shells, locks and floor each printed separately and then assembled by hand. Stops were printed separately and similarly glued on using Gorilla Super Glue Gel.

Bambu Studio was used as the slicer. Besides filament and the occasional addition of tree supports, no settings were changed to keep as much consistency across printed models as possible.

In order to develop the prototypes and display the usage of 3D printing in refining and confirming viability, a total of four tests were conducted:

1. Clearance and folding thickness (telescoping and Miura models, respectively)
2. Collapsed-versus-expanded dimensions
3. Deployment time & reliability

Two mechanism-specific tests were conducted: one for each of the prototypes, focusing on a pressing or significant variable that might affect a final engineering solution. For the telescoping mechanism, this test specifically looked at the clearance for the rail utility and between the shells themselves. For the Miura model, the test looked at the thickness and design of the flexible living hinge between adjacent panels.

These mechanism-specific tests, taking place at small-scale printed specimen level, were the primary tests used for iteration and to refine the designs of each mechanism. These tests confirmed and finalized the most optimal design of each mechanism and allowed for full prototype printing. This shows the ability and accessibility of 3D printing in design iteration and refinement. Then, these optimized full-mechanism tests underwent two more controlled experiments, which were designed to display geometric behaviors that would mirror a large prototype, and showed the ability of 3D printing to model viability and limitations of design concepts. These tests also showed the specific workings and behaviors of the two collapsible methods chosen.

The first non-iterative experiment measured how effectively each model reduced its occupied space. The model's volume was calculated in both its deployed and compact states. An approximate percentage reduction and deployment ratio were then calculated using these measurements.

The second non-iterative experiment measured how quickly and how reliably the mechanism deployed. Deployment time was measured to examine how easily and consistently each mechanism moved between configurations. Using a smartphone video for the most accuracy, each model was expanded or compressed across multiple tests. Mean time, minimum time, maximum time, number of successful trials, and observed difficulties were reported for each model.

4.2.1 Iterative Telescoping Test

The mechanism-specific tests were the most-used tests in the early stages of prototype development. Because the prototypes were tested small-scale first before fully assembling for the remaining three tests, these mechanism-specific tests were recorded in order to provide very quick improvements to ensure that the final product would operate smoothly.

For the telescoping mechanism, the two most pressing clearances are the gap between the nested shells and the rail clearance:

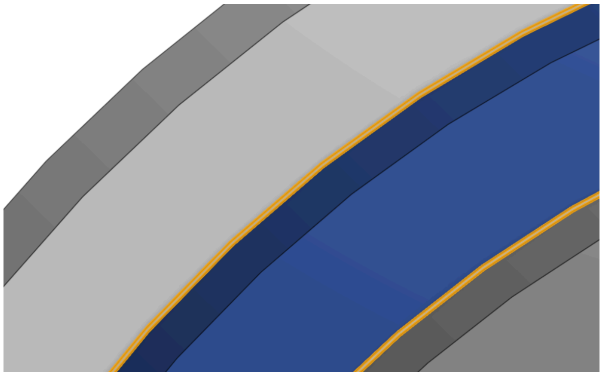

Fig6. Clearance between shells

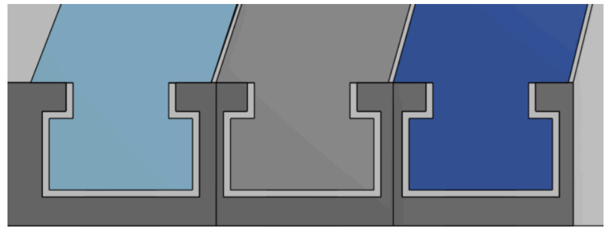

Fig7. Rail clearance

The most suitable clearance was defined as the smallest value that permitted complete movement without frequent binding, while maintaining acceptable alignment. The selected value was then incorporated into the next complete telescoping prototype. This iterative test had two stages: the first consisted of testing the clearance with the rails, and the second consisted of testing the clearance with the shells.

In the first stage, short rail-and-slider models were printed to isolate the effect of clearance without requiring an entire telescoping model for each trial. Only the designed gap between the sliding surfaces was changed; otherwise, all other variables remained constant.

Sliding resistance was estimated using an incline test. One end of the rail specimen was slowly raised until the rail began to move downwards, and the angle at which the movement began was measured using a smartphone inclinometer. A lower angle indicated lower resistance to movement.

Lateral looseness was measured by tilting the slider as far as the rail would allow and measuring the angle from vertical that the slider was able to tilt. Since the slider was vertical for the purposes of the test, not curved like the shells, the angle was measured from the center of the slider (which was drawn with a line) and a freestanding pin to serve as complete vertical reference. This test also utilized a smartphone inclinometer. In this case, a lower angle indicated lower lateral play.

Clearance values of .1 mm, .25 mm, .4 mm, .55 mm, and .7 mm were tested. Each test was repeated three times for each model. The graphs below display the data trend plotted using the mean; error bars represent the standard deviation (±1 standard deviation was used).

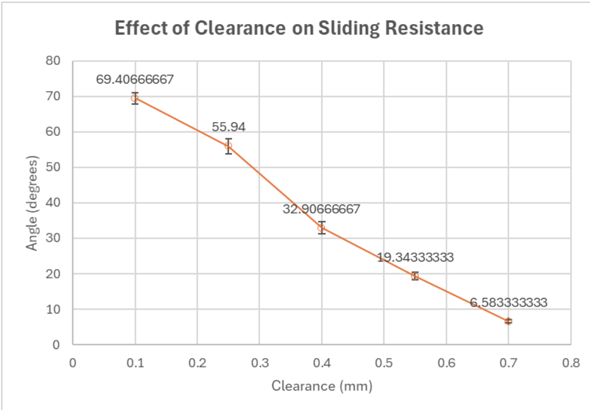

Fig8. Effect of Clearance on Sliding Resistance

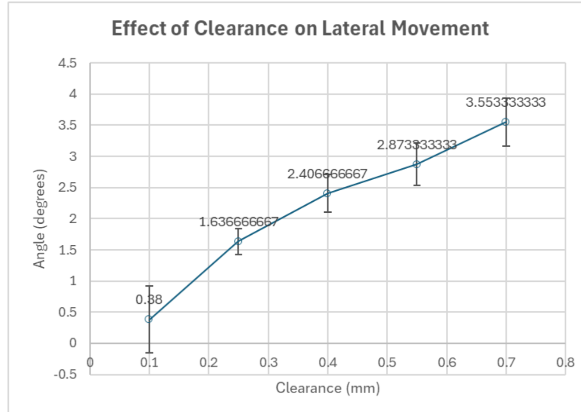

Fig9. Effect of Clearance on Lateral Movement

In the second stage, two shells (the smallest two) were printed on rails with .4 mm clearance based on the results from the previous stage. The larger shell stayed the same throughout all tests, while the smaller shell's size differed slightly based on the clearance set between the two shells. The time taken to successfully fit the smaller shell into the larger shell was recorded using smartphone video to achieve greater timing accuracy, with notes on difficulty and whether extra force was required. This test was repeated three times.

Clearance values of .1 mm, .25 mm, .4 mm, and .55 mm were tested for the clearance. The graph below displays the results, using the mean ±1 standard deviation:

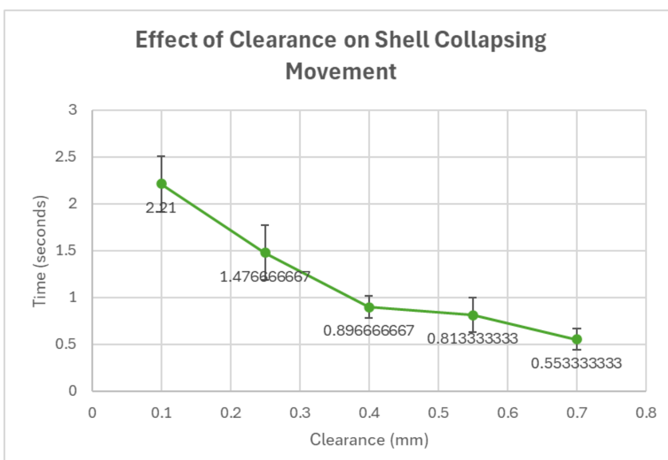

Fig10. Effect of Clearance on Shell Collapsing Movement

It was found that at .1 mm, significantly more force was required compared to at .25, .4, and .55 mm, while .55 mm achieved a very loose fit, with the inner shell able to move significantly around once collapsed inside. .4 mm similarly produced a loose fit

Based upon the outcome of these two testing stages, a rail clearance of .4 mm was selected. A clearance value of .25 mm was selected for the clearance between shells.

4.2.2 Miura Iterative Test

This test centered on the flexible connection between panels and how, ultimately, an entire prototype of hundreds of connecting panels could sustainably be connected using PETG, while still being able to fold enough to compress. This test proceeded in two stages: in the first stage, each specimen contained two identical rigid panels connected by one flexible PETG fold region. The thickness of the fold region was varied to see which fold thickness provided the greatest flexibility while still providing durability. The second stage consisted of a series of rapid iterations, gradually expanding the number of panels until the full prototype was reached, using the thickness found in stage one.

For the first stage, the tests were conducted using specimens of two rectangular rigid panels (9x11 mm) with a flexible region of 5 mm in between. Only the thickness of the flexible region was changed; all other variables remained constant. Fold thicknesses of .1, .3, .5, .7, and .9 millimeters were tested, with one specimen at each thickness.

Each specimen was first folded until the two flat panels were able to touch or until the furthest the specimen could fold without cracking or separating along the print layers. Then, the specimens completed repeated bending cycles. One cycle consisted of moving from the flat position to the target fold angle (the two flat panels touching) and returning to the flat position. The specimens were inspected every ten cycles for cracking, whitening, separation of layers, or complete breakage. The angle was determined using a smartphone inclinometer.

Testing continued until the specimen completed 40 cycles or experienced a defined failure. Failure was defined as a visible crack, complete layer separation, and/or inability to maintain connection between the panels.

The table below summarizes the results obtained from this test:

Fold thickness (mm)	Mean fold rotation (±1 standard deviation)	Cycles before failure
.1	179.46 ± 1.66	23
.3	174.12 ± 2.03	N/A
.5	162.75 ± 4.21	N/A
.7	143.11 ± 4.02	N/A
.9	119.56 ± 2.54	N/A

The test then moved into stage two, which involved printing a four-panel configuration, which is a complete Miura unit. To begin with, only one unit was printed with a .3 mm thickness to

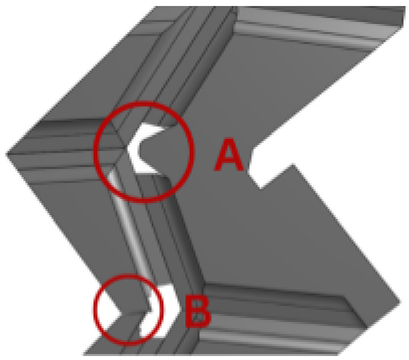

Fig11. Closeup

investigate how one complete unit would behave after being printed, and if any changes needed to be made to the design itself. It was found that the panels all being connected made it difficult to fold the unit into a flatter configuration, as the material in the center would interfere. In order to encourage better folding, a gap was created (in the center between the four panels), shown at point A in the figure to the left. A second printed unit confirmed that this change created a more robust unit; it achieved a much flatter folded state.

The most viable thickness for the fold region was .3 mm, so three four-panel configurations were printed: one with all .25 mm connections, one with .3 mm connections, and a last with .35 mm connections.

The same tests were conducted with 60 cycles since the difference between the thicknesses was smaller.

Fold thickness (mm)	Mean fold rotation (±1 standard deviation)	Cycles before damage
.25	178.89 ± 0.91	N/A
.3	175.34 ± 3.11	N/A
.35	175.54 ± 2.36	N/A

Afterwards, based on this data, an entire chain was printed with a .28 mm connection. To promote better folding based on the results of this full chain, an actual gap was added between adjacent units, shown at point B. A new chain was produced using this iteration. The tab-gluing connection was then tested with another chain, and following the success of both of these iterations, the full-scale prototype was assembled.

4.3 Collapsed vs Expanded Dimensions Test

For this test, each prototype was first placed in its fully expanded configuration on a flat surface. Its dimensions were measured using a ruler, and it was then placed in its most compact intended configuration, and the same measurements were repeated. The measurements were taken three times each (the exact measurements taken on each mechanism are detailed below), and the mean of each was taken.

Using those measurements, the volume of each mechanism when expanded and collapsed was taken. Note that the measurements taken were bounding measurements, so the volume cannot be claimed to be completely accurate; for the purposes of the test, however, the volumes provided a consistent model-scale measurement of compactness. The percentage reduction in occupied volume and the deployment ratios were calculated based on these volumes.

The Miura prototype's volume was calculated using the volume of a cylinder. Therefore, the measurements taken were of the bounding diameter and the height in the expanded and collapsed versions. The Miura model achieved an 89.889% volume reduction and an 8.999 (9):1 deployment ratio (collapsed bounding volume of 31.172 cubic cm, expanded bounding volume of 280.552 cubic cm).

The telescoping prototype's volume was calculated using three-dimensional semicircle volume principles. Therefore, the measurements taken were of the radius of each shell; the area of the semicircle was calculated, then multiplied by the thickness of each shell (33 mm each). This model achieved a 68.004% volume reduction and a 3.125:1 deployment ratio (collapsed bounding volume of 725.808 cubic cm, expanded bounding volume of 2268.406 cubic cm).

4.4 Deployment Time Reliability Test

Deployment time was measured to examine how easily and consistently each mechanism moved between configurations. A smartphone video was used in order to more accurately define time instead of relying on a manually operated smartwatch. The model was both collapsed and expanded, and the time taken to do so was recorded. The time taken to lock each mechanism was included in this time, including the Miura latching pins and folding the floor up for the telescoping model. Each prototype completed fifteen expansion tests and fifteen collapsing tests; along with the time, failure or success to fully deploy was also recorded. In this test, a successful deployment was defined as one in which the model reached the final configuration without any breakage or without needing the trial to be restarted for any reason.

About 3 trial runs of both expansion and collapsing were completed at the beginning to determine the approximate level of force required to initiate both actions on either mechanism.

Finally, any need to repeat part of the movement or overtly guide movement was recorded, even if the final deployment was successful. This allowed further insights into the mechanism's reliability as well as complexity. Because these prototypes were not motor-powered, the investigator would manually initiate deployment or collapsing, so overt guidance was defined as a need for repetition, a need to apply extra force beyond what was initially applied, or a need to manually interface with other parts of the mechanism. These 'other parts' meant parts not directly involved with expansion or collapsing that might have interfered with motion.

Overall, mean time, minimum time, maximum time, success rate, and additional notes were recorded. The graph shows the mean time and ±1 standard deviation:

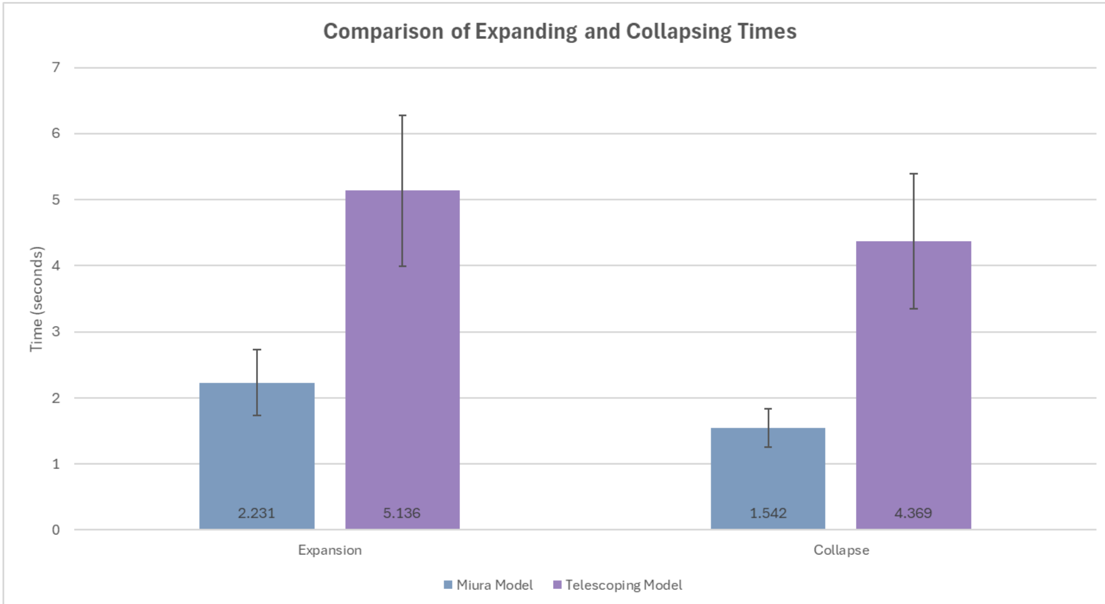

Fig12. Comparison of Expanding and Collapsing Times

Of the fifteen expansion trials, the Miura model and the telescoping model both achieved a 100% success rate. Of the fifteen collapsing trials, the Miura model experienced an 86% success rate, and the telescoping model experienced a 100% success rate.

Additional notes include an observation that the telescoping model typically required more overt guidance to deploy (about four times out of fifteen compared to the Miura model's two), while the Miura model began to show noticeable wear (white stress lines in some locations, particularly at the tabs connecting the top of each chain to the lid) at trial 7 of the collapsing trials. Furthermore, the Miura model began to show signs of resistance at trial 9 of the collapsing trials, requiring additional force to collapse.

5. Discussion

5.1 Findings and Comparisons of Prototypes

The results demonstrate that both the telescoping and Miura-inspired concepts can produce a collapsible form at a small scale. However, the two prototypes achieved this through very different mechanical behaviors and therefore presented different advantages and limitations. The telescoping design generally favored reliability and controlled movement, whereas the Miura-inspired design enabled faster, more coordinated deployment but showed greater vulnerability and stress during repeated collapse.

For the telescoping mechanism, the clearance experiments demonstrated the expected compromise: a suitable clearance would need to be chosen to make sure that there was enough room to move properly, but not too much to encourage excessive lateral play. A comparable tradeoff appeared in the Miura fold-thickness experiment: the fold thickness needed to be thick enough to sustain repeated folding, but thin enough to allow flexible collapsing movement.

A notable insight is that the Miura model took much more iteration, printing, and CAD work to ultimately reach the final product, due to the inherent challenge presented by origami-inspired thick structures. Particularly: the telescoping mechanism produced the expected horizontal sliding motions with all clearances, while the Miura mechanism, during the smaller tests, did not always produce the expected vertical folding motion. As such, more printing and testing were needed to change the geometry, shown with the widening of the gap in the center and the gap between adjacent units.

The complete prototypes revealed additional trade-offs that were not as visible in the component tests. Both prototypes showed the ability to successfully collapse, while the Miura model proved to be more space-efficient, with almost a 90% reduction in volume, compared to about 68% for the telescoping model. As for deployment, the telescoping prototype took considerably longer to deploy in both directions (2.905 seconds longer in expansion, 2.827 seconds longer in collapse) and had a greater standard deviation (.566 greater in expansion, .75 greater in collapse) than the Miura prototype. The longer and less consistent times are likely connected to the need to move several nested shells; the Miura model collapsed in a single degree of freedom.

However, it was outperformed by the telescoping mechanism in terms of durability, notably that it had a lower success rate for collapse (86%, compared to 100%). Stress lines also began to appear around some connecting tabs during the seventh collapse trial due to the repeated folding. Although the prototype continued functioning, the visible stress marks may represent an early stage of fatigue and identify an area requiring further redesign.

Overall, the Miura mechanism offered faster and more coordinated deployment, while the telescoping mechanism completed the trials more reliably but required more time and guidance. For an application in which rapid deployment is the main priority, the Miura approach may be more promising; and if predictable positioning and collapse reliability are more important, a telescoping system may provide advantages. Note that these conclusions only concern the mechanisms demonstrated by the prototypes rather than complete housing systems.

5.2 The Contribution of Small-Scale 3D Printing

The experiments show that one of the main contributions of small-scale 3D printing is its ability to support rapid and focused design iteration. Instead of immediately manufacturing complete prototypes, individual design variables could first be tested using smaller specimens: the rail-and-slider models isolated the effect of clearance in the telescoping mechanism, while the two-panel specimens isolated the effect of fold thickness in the Miura mechanism.

The Miura prototype provides the clearest example of this iterative process, which is logical considering this was a much more challenging design to print based on the many connections (as mentioned above). Development progressed from a two-panel fold specimen to a four-panel unit, then to a connected chain and finally to a complete prototype. At each stage, a different problem became visible: the two-panel folds revealed optimal and feasible hinge thickness; the four-panel models exposed interference around the center gap and connecting tab; the chain models showed the need for additional spacing between units. Similarly, the telescoping clearance tests transformed a general design problem into a measurable engineering decision, identifying a tradeoff between sliding resistance and lateral stability; thus narrowing the feasible rail-clearance range for the complete prototype. Overall, 3D printing allowed identification of important design parameters and revealed tradeoffs between competing objectives inexpensively and quickly.

It is important to note that the specific clearances and values obtained from these first two iterative tests cannot be said to be accurate for a larger model or a final product, even if proportionally scaled to other parts. The first two iterative tests can be appropriately classified as design-parameter sensitivity experiments: they show how small-scale printing can identify important variables and guide the next prototype. The two full-model tests then determine whether those selected parameters remain effective after being integrated into a more complicated system. These two tests then provided valuable information on both designs and principles of collapsible housing, as outlined above.

Then, the full-model tests supported the hypothesis that 3D printing was able to reveal the feasibility and robustness of the telescoping and origami geometries. It revealed important movement and component interactions, like the need for the telescoping mechanism to require extra assistance as well as the Miura mechanism's tendency to stress lines and fail more often. It was able to create direct comparisons between the two designs, namely their efficiency in collapsing volume and collapsing speed, as well as durability comparisons. As such, while 3D printing was unable to accurately assess the strength, durability, and complete interactions between components that a full-scale prototype could, through the tests it was able to reveal important information and comparisons about the two designs.

5.3 Limitations

This study has several limitations. Most importantly, the prototypes were small mechanical models rather than structurally complete houses. Successful movement at model scale does not demonstrate that the same mechanisms would work at architectural scale, as enlarged components would naturally interface differently. The structures also did not represent occupiable structures or complete housing systems, and did not include necessary components for habitation; instead, they looked at specific geometries in early development.

Material selection created another limitation. Neither material (PLA nor PETG) can fully accurately represent the real materials that would be required in a full-sized structure. Because the telescoping model used PLA and the folding model used PETG, differences between their performances cannot be attributed solely to either the mechanisms or the materials.

Finally, the experiments involved a limited number of models and tools, and manually operated trials. Deployment time and reliability may have been affected by human error in operating trials and recording data. Short repeated-cycle tests could identify early wear but could not predict long-term fatigue, and measurements of collapsed volume were also approximate because they used bounding-box dimensions rather than the exact occupied volume.

These limitations mean that the results should be interpreted as early-stage design evidence. The prototypes were most useful for identifying geometry behavior, design tradeoffs and parameters, and comparisons between designs, which should all be examined through larger and more controlled future studies. Importantly, the prototypes and iterations still showed the value of 3D printing in prototyping and may also serve to provide important information on collapsible housing.

References

[1] Ngo, T. D., Kashani, A., Imbalzano, G., Nguyen, K. T. Q., & Hui, D. (2018). Additive manufacturing (3D printing): A review of materials, methods, applications and challenges. *Composites Part B: Engineering*, 143, 172–196. https://doi.org/10.1016/j.compositesb.2018.02.012

[2] Cerrahoğlu, M., & Maden, F. (2024). Design of transformable transitional shelter for post-disaster relief. *International Journal of Disaster Resilience in the Built Environment* 15(2), 227–243. https://doi.org/10.1108/IJDRBE-05-2022-0049

[3] Verzoni, A., & Rais-Rohani, M. (2022). Transition analysis of flat-foldable origami-inspired deployable shelter concepts. *Engineering Structures*, 273, 115074. https://doi.org/10.1016/j.engstruct.2022.115074

[4] Kim, T. H., *et al*. (2025). Construction of metre-scale foldable space shelter based on gravity-driven self-assembling origami. *Scientific Reports*. https://www.nature.com/articles/s41598-025-04241-8

[5] Ye, H., Liu, Q., Cheng, J. *et al.* Multimaterial 3D printed self-locking thick-panel origami metamaterials. *Nat Commun* 14, 1607 (2023). https://doi.org/10.1038/s41467-023-37343-w

[6] Sun, C., Li, D., Liao, W., Liu, T., Zhang, C., & Xiong, Y. (2026). High-load-bearing and ultra-wideband absorbing reconfigurable Miura-ori metastructures. *Composites Science and Technology, 281*, 111658. https://doi.org/10.1016/j.compscitech.2026.111658

[7] Martins, R. F., Branco, R., Martins, M., Macek, W., Marciniak, Z., Silva, R., Trindade, D., Moura, C., Franco, M., & Malça, C. (2024). Mechanical properties of additively manufactured polymeric materials—PLA and PETG—for biomechanical applications. *Polymers*, 16(13), 1868. https://doi.org/10.3390/polym16131868